Tin oxide micro/nano fibers from electrostatic deposition

Y. Wang[1,a], M, Aponte[2,b], N. León[2], I. Ramos[2], R. Furlan[2], N. Pinto[2], J.J. Santiago-Avilés[1]
[1]*Dept of Electrical & Systems Engineering, Univ of Pennsylvania, Philadelphia, PA 19104, USA.*
[2]*Dept of Physics & Electronics, Univ of Puerto Rico at Humacao, CUH Station, Humacao, PR 00791.*

Recibido el 27 de octubre de 2004; aceptado el 26 de mayo de 2005

SnO_2 micro/nano fibers in the rutile structure were synthesized using electrospinning and metallorganic decomposition techniques. Fibers were electrospun using two different precursor solutions, one based on $SnCl_4$ and the other on $C_{22}H_{44}O_4Sn$. The fibers were sintered in air for two hours at 400, 500, 600, 700 and 800°C. SEM, AFM, XRD, XPS and Raman microspectrometry were used to characterize the sintered fibers. The results showed that the fibers were composed of SnO_2 and that the $SnCl_4$ precursor led to better results in terms of uniformity/continuity of the fibers.

Keywords: Tin oxide; nanofibers; electrospinning.

Micro/nano fibras de SnO_2 rutilo se sintetizaron con electrospinning y técnicas de descomposición metalo-orgánicas. Las fibras se produjeron utilizando dos soluciones precursoras distintas basadas en una mezcla de $SnCl_4$ y otra de $C_{22}H_{44}O_4Sn$. Las fibras se quemaron en aire por dos horas a temperaturas de 400, 500, 600, 700 y 800°C y se analizaron utilizando SEM, AFM, XRD, XPS y microscopía Raman. Los resultados muestran que las fibras producidas con ambos precursores están compuestas de SnO_2 y que la solución precursora con $SnCl_4$produce fibras más uniformes y continuas.

Descriptores: Óxido de estaño; nanofibras; electrospinning.

PACS: 81.16.Be; 81.15.Pq; 61.82.Fk

1. Introduction

Tin oxide, SnO_2 is an n-type semiconductor with a large bandgap (E_g=3.6eV at 300K). The use of SnO_2 thin films as chemical sensors for environmental and industrial applications has been studied intensively [1-3]. SnO_2 in the form of fibers is expected to have improved chemical sensing characteristics [4]. The effective surface area for sensor applications depends on the total grain boundary (GB) area in the SnO_2 sensing element. The GB area-to-volume ratio will increase with the reduction in grain size. If we can fabricate the element in the form of fibers with their diameter on the nano scale, the grain size will be reduced due to restriction the grain growth along the cross-section of the fibers, and fibers are expected to be more sensitive than a thin film. Efforts to synthesize the structures include the development of nanofibers, nanowires, nanorods, and nanobelts [5-10]. Of the methods used to produced the nanostructures, electrospinning is especially interesting in that it is easy and cost effective [6,8,9].

As the active element in chemical or biological sensors, the tin oxide nanofibers can be configured either as resistors whose conductance is altered by charge-transfer processes occurring at their surfaces, or as field-effect transistors whose properties can be controlled by applying an appropriate potential to their gate [11]. The conductivity of the SnO_2 semiconductor is modulated by the chemisorbed oxygen molecules on its surface. The absorbed oxygen, receiving electrons from the conduction band, produces an electron depletion layer under the absorbing surface and a potential barrier between particles, and thus decreases the conductivity of the SnO_2 [4]. This makes SnO_2 a good candidate as a gas sensor whose conductivity will increase sharply when exposed to a reducing gas. Sensors based on SnO_2 wires using the conductance or field effect transistor configuration have been reported [10-12] with good electrical and photoconduction properties.

2. Formation process

Fibers were electrospun from two simple precursor solutions. For both solutions, the viscosity was controlled using a solution of poly(ethylene oxide) (PEO) [-CH_2CH_2O-]n (molecular weight 900,000 Aldrich) and chloroform ($CHCl_3$ Sigma). The $SnCl_4$ solution [8] was prepared using anhydrous tin(IV) chloride ($SnCl_4$ ACROS Organics), deionized water, propanol (C_3H_7OH, Fischer Scientifics), and isopropanol (2-C_3H_7OH, Fischer Scientifics) $SnCl_4$:H_2O:C_3H_7OH:2-C_3H_7OH in the following molar ratio: 1:9:9:6. Then the $SnCl_4$ solution was combined with the viscous solution (200 mg PEO/10 ml $CHCl_3$) at a volume ratio of 1:1.25. The $C_{22}H_{44}O_4Sn$ solution [9] was made using liquid dimethyldineodecanoate tin combined with the viscous solution (100 mg PEO/10 ml $CHCl_3$) at a volume ratio of 2:1. The fibers were produced using a simple electrospinning setup, described in more detail elsewhere [13], followed by sintering using a resistance furnace with a Sentry 2.0 digital temperature controller made by Paragon Industries, Inc.

3. Characterization

SEM and SPM observations revealed that the horizontal diameter of sintered fibers ranges from 60 nm to 10μm. Figure 1 shows a typical image of a single fiber. Figure 2 shows the SPM apparent average cross-section profile. It is a distortion of the actual profile because the tip not only has its own cone shape and size, but also cannot trace the lower part of the fiber. However, the vertical dimension (diameter) of 100 nm is not distorted and is therefore accurate. The SEM and SPM analysis indicates that the $SnCl_4$ precursor led to better results in terms of uniformity/continuity of the fibers.

Figure 3 shows the XRD spectra for fibers electrospun using the $SnCl_4$ precursor. After sintering at 400°C, 110, 101 and 211 XRD peaks of rutile structure SnO_2 appear, indicating the formation of its recipient lattice. These peaks become more distinct and an additional 200, 220 and 310 peaks showed up after sintering at 600°C, indicating the development of a more integral rutile lattice between 400°C and 600°C. Up to 800°C, all peaks are still identified as SnO_2 peaks, suggesting the following overall chemical reactions:

$$\mathrm{Sn(OH)}_n\mathrm{Cl}_{4-n} + (4-n)\mathrm{H_2O} \rightarrow \mathrm{SnO_2} + 2\mathrm{H_2O} + (4-n)\mathrm{HCl}, \quad (1)$$

$$[-\mathrm{CH_2CH_2O}-]_n + (5n/2)\mathrm{O_2} \rightarrow 2n\mathrm{CO_2} + 2n\mathrm{H_2O}, \quad (2)$$

and $n = 0$, 1, 2, 3, 4.

For sintering temperatures of 400, 600 and 800°C, the relative intensities of the diffraction peaks are consistent with those reported in Ref. [14].

Typical Raman micro-scattering spectra are presented in Fig. 4. After sintering at 400°C, a peak around 631cm^{-1} shows up, whereas another weak peak centered around 774cm^{-1} begins to appear. The two peaks become more distinct after sintering between 600 and 800°C, whereas the third peak appears around 474 cm^{-1} after sintering at 800°C. The SnO_2 rutile structure belongs to the space group

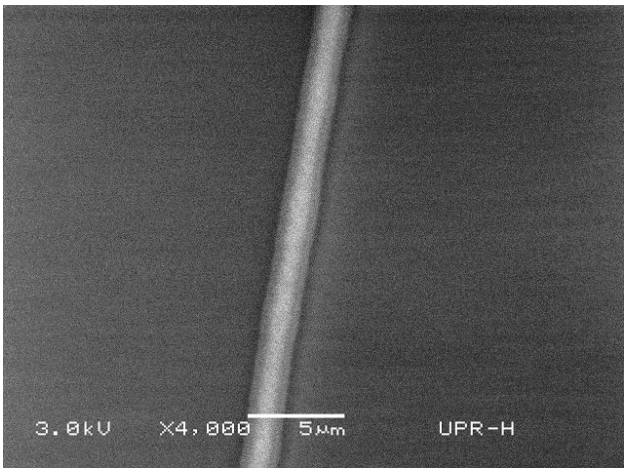

FIGURE 1. SEM micrograph of a single fiber sintered at 600°C for 2 hours.

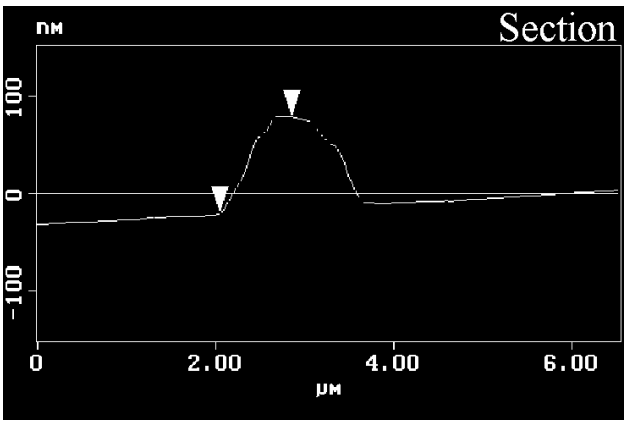

FIGURE 2. SPM apparent average cross-section profile of a single fiber sintered at 600 °C for 2 hours.

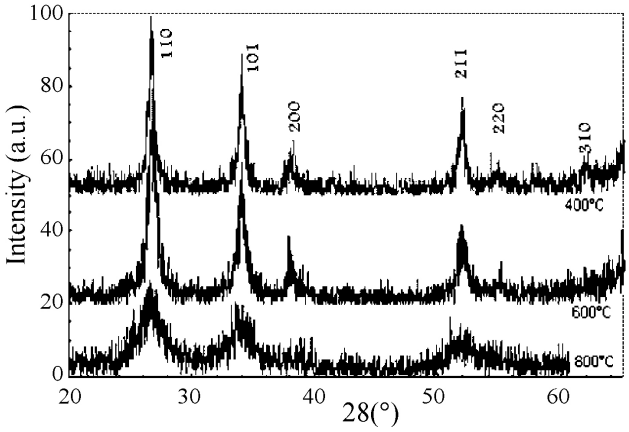

FIGURE 3. XRD Spectra for $SnCl_4$-based fibers at different temperatures.

$P4_2/mnm$ [15]. Its normal lattice vibration at the Γ point of the Brillouin zone is

$$\Gamma = 1\mathrm{A}_{1g} + 1\mathrm{A}_{2g} + 1\mathrm{A}_{2u} + 1\mathrm{B}_{1g} + 1\mathrm{B}_{2g} + 2\mathrm{B}_{1u} + 1\mathrm{E}_g + 3\mathrm{E}_u. \quad (3)$$

Of the 11 optical phonons of symmetry, A_{1g}, B_{1g}, B_{2g}, and E_g are Raman active with the strongest Raman intensity at 631.3cm^{-1} for mode A_{1g}, followed by the mode B_{2g} at 774.4cm^{-1} and the mode E_g at 474.0cm^{-1} (B_{1g} peak is centered at 87$\pm$2cm^{-1}). The peak position and relative intensity of A_{1g}, B_{2g} and E_g modes are in agreement with those observed in a large ($\sim$1cc) natural cassiterite crystal [15] or synthesized SnO_2 nanorods [5]. It is noteworthy that after sintering at 800°C, two peaks appear around 605 and 708 cm^{-1}. They cannot be attributed to any mode of lattice vibration in rutile SnO_2, implying a subtle structure change that XRD is not so sensitive to detect.

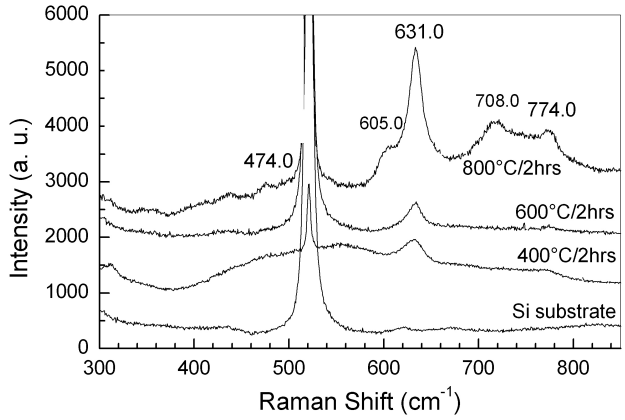

FIGURE 4. Raman micro-spectra of Si substrate and $SnCl_4$-based mats sintered at different temperatures.

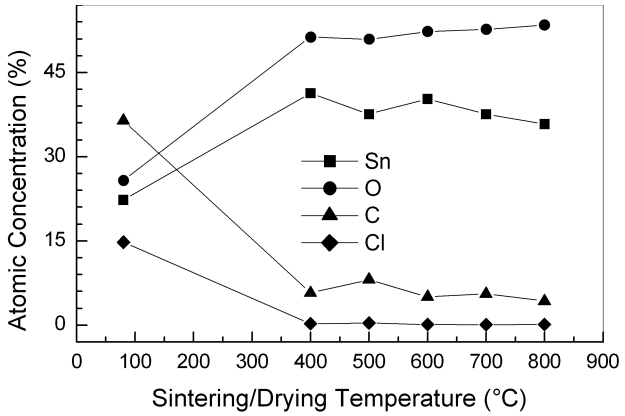

FIGURE 5. Sintering temperature dependence of the atomic concentration of $SnCl_4$-based fibers.

The XPS spectra indicated the existence of elements Sn, O, C and Cl, as well as Si in sintered mat samples [16]. The XPS spectra for the Sn, O, C and Cl regions give the relative intensity of the elements as a function of the binding energy for mats sintered at 400, 500, 600, 700 and 800°C. Using the atomic sensitivity factor, the relative atomic concentrations of Sn, O, C and C were analyzed semi-quantitatively and their dependence on the sintering temperature is shown in Fig. 5. Upon sintering at 400°C, Cl almost disappears; C concentration decreases sharply from 36.4% to 5-8%, whereas O concentration increases to more than 50%, and Sn concentration increases to 38%.The drastic decrease of carbon concentration and the regular shift of the XPS C1s peak caused by sintering suggest that the carbon is a residual element rather than an adventitious extrinsic impurity. We are currently investigating the properties of the sintered tin oxide fibers and their dependence on the preparation conditions and shall report the results in a coming paper.

4. Conclusion

Tin oxide (SnO_2) fibers, in the rutile phase with diameters ranging from 60nm to several microns were synthesized using two different precursor solutions. The first was a mixture of $C_{22}H_{44}O_4Sn$, and the second a mixture of $SnCl_4$ sol. In both cases the viscocity was controlled using a poly(ethylene oxide) (molecular weight 900,000)/chloroform solution. The fibers were fabricated using electrospinning and metallorganic decomposition techniques. Scanning electron microscopy, scanning probe microscopy, x-ray diffraction, Raman microspectrometry and x-ray photoelectron spectroscopy were used to characterize the sintered fibers. The results showed that a series of chemical reactions resulted in SnO_2 fibers in rutile structure at sintering temperatures between 400 and 700°C, and that the $SnCl_4$ precursor led to better results in terms of uniformity/continuity of the fibers.

Acknowledgements

This work was supported by NSF-DMR-353730 and NSF-SBE-0123654.

[a] Current address: Dept of Electrical and Computer Engineering, Univ of California, Davis, CA, 95616.

[b] Current address: Dept of Materials and Ceramics Engineering, Rutgers Univ, NJ, USA.

1. J. Watson, *Sensors and Actuators* **5** (1984) 29.
2. W. Gopel and K.D. Schierbaum, *Sensors and Actuators B* **26** (1995) 1.
3. A. Tang *et al.*, *Sensors and Actuators B* **43** (1997) 161.
4. S. Seal and S. Shukla, *Journal of Metals* **54** (2002) 35.
5. C. Xu, G. Xu, Y. Liu, X. Zhao, and G. Wang, *Scriptia Materialia*, **46** (2002) 789.
6. D. Li, Y. Wang and Y. Xia, *Nano Letters* **3** (2003) 1167.
7. M. Law, J. Goldberger and P. Yang, *Annu. Rev. Mater. Res.* **34** (2004) 83.
8. Y. Wang *et al., Journal of the American Ceramics Society* (2005) in press.
9. Y. Wang *et al.*, *Semicond. Sci. Techn.* **19** (2004) 1057.
10. E. Comini *et al.*, *Applied Physics Letters* **81** (2002) 1869.
11. A. Kolmakov and M. Moskovits, *Annu. Rev. Mater. Res.* **34** (2004) 151.
12. P. Candeloro *et. al., Microelectronic Engineering* **78** (2005) 178.
13. Y. Wang, R. Furlan, I. Ramos and J.J. Santiago-Avilés, *Applied Physics A* **78** (2004) 1043.
14. JCPDS Card No. 41-1445.
15. J.F. Scott, *J. Chem Phys* **53** (1970) 852.
16. J.F. Moulder *et al.*, *Handbook of X-Ray Photoelectron Spectroscopy*, Jill Chastain, (by Perkin-Elmer Corporation, Physical Electronics Division, Minnesota, USA, 1992).